November 2016

Trypanosoma Brucei Mitochondrial DNA POLIB Cell Cycle Localization and Effect on POLIC when POLIB is Depleted

Sylvia L. Rivera
University of Massachusetts Amherst

TRYPANOSOMA BRUCEI MITOCHONDRIAL DNA POLIB CELL CYCLE LOCALIZATION AND EFFECT ON POLIC WHEN POLIB IS DEPLETED

A Thesis Presented

By

Sylvia L. Rivera

Submitted to the Graduate School of the
University of Massachusetts Amherst in partial fulfillment
of the requirements for the degree of

MASTER OF SCIENCE

September 2016

Department of Microbiology

TRYPANOSOMA BRUCEI MITOCHONDRIAL DNA POLIB CELL CYCLE LOCALIZATION AND EFFECT ON POLIC WHEN POLIB IS DEPLETED

A Thesis Presented

By

Sylvia L. Rivera

Approved as to style and content by:

_____
Michele Klingbeil, Chair

_____
Yasu Morita, Member

_____
Steve Sandler, Department Head and Member
Department of Microbiology

ABSTRACT

TRYPANOSOMA BRUCEI MITOCHONDRIAL DNA POLIB CELL CYCLE LOCALIZATION AND EFFECT ON POLIC WHEN POLIB IS DEPLETED

September 2016

SYLVIA L. RIVERA

B.S. UNIVERSITY OF PUERTO RICO MAYAGUEZ

M.S. UNIVERSITY OF MASSACHUSETTS AMHERST

Trypanosoma brucei is the causative agent of Human African Trypanosomiasis (HAT), also known as African sleeping sickness. *T. brucei* is unique in several ways that distinguish this organism from other eukaryotes. One of the unique features of *T. brucei* is the organism's mitochondrial DNA, which is organized in a complex structure called kinetoplast DNA (kDNA). Since kDNA is unique to the kinetoplastids, kDNA may serve as a good drug target against *T. brucei*. Previews studies have shown that kDNA has 4 different family A mitochondrial DNA polymerases. Three of these mitochondrial DNA polymerases (POLIB, POLIC, and POLID) are essential components of kDNA synthesis and replication. POLID and POLIC dynamically localize throughout the cell cycle. POLID is found dispersed in the matrix before the kDNA has undergone replication and is re-localized at the antipodal sites when the kDNA is dividing. POLIC is found in the

kinetoflagellar zone (KFZ) at low concentrations when the kDNA is not replicating and relocalizes to the antipodal sites when dividing. Based on the dynamic localization of these two DNA polymerases, we hypothesize that POLIB undergoes dynamic localization at some point during the cell cycle stage. Here, a POLIB/PTP single expressor cell line was analyzed by immunofluorescence microscopy in an unsynchronized population. We characterized the localization pattern of POLIB-PTP at different cell cycle stages and found different localization patterns throughout cell cycle. Cells at 1N1K (the majority of cell in an unsynchronized population) have single foci, but at $1N1K_{div}$ two different patterns are mainly observed, diffuse and segregated. When the kDNAs are separated POLIB-PTP is again seen as a distinct foci in each kDNA. By doing TdT labeling and a quantitative analysis, we found that at early stages of minicircles replication POLIB-PTP start relocalizing to the kDNA disk with a diffuse pattern being the main. By the time the minicircles are being reattached in the disk (late TdT), POLIB is seen in the disk as a bilobe shape.

TABLE OF CONTENTS

Page

ABSTRACT ……..iii
LIST OF TABLES ……..vii
LIST OF FIGURES……..……viii
CHAPTER
1. INTRODUCTION ……..……..1
1.1. Trypanosoma brucei ……..……....1
1.2. kDNA Structure ……..…….....2
1.3. kDNA replication and cell cycle progression ……..…..4
1.4. Rationale and objective ……..……7
2. MATERIALS AND METHODS ……....10
2.1. Plasmid constructs ……..……..……10
2.1.1. POLIB-PTP chromosomal tagging construct ……..…….10
2.1.2. POLIB knockout construct ……..…10
2.2. Trypanosome growth and cell lines ……..……12
2.2.1. Standard growth conditions ……....12
2.2.2. Generation of TbIB-PTP single expressor cell line ……..12
2.2.3. POLIC chromosomal tagging and POLIB RNA interference ……..12
2.3. Fluorescence Microscopy ……..……13
2.3.1. Immunofluorescence (IF) ……..……13
2.3.2. In situ TdT labeling and quantification ……14
2.4. Image acquisition and analysis ……..……14
2.4.1. Microscope and software ……..……14
2.4.2. Plot profile analysis ……..….15
2.4.3. Surface plot analysis ……..……15
2.5. Western Blot ……..….15
2.6. Cycloheximide Treatment ……..16

2.7. POLIB RNAi ……..16
2.7.1. Cell Growth ……..……...16
2.7.2. RNA isolation and Reverse-Transcription Quantitative PCR …….17
3. RESULTS ……...……..19
3.1. POLIB-PTP is seen in all cell cycle stages ……..….19
3.2. POLIB-PTP does not localize at the antipodal sites ……..……22
3.3. Depletion of POLIB causes a reduction of POLIC-PTP …… 24
4. DISCUSSION ……..….38
REFERENCES ……43

LIST OF TABLES

Table Page

1.1 Current treatments for human African trypanosomiasis …….....3

1.2 Trypanosoma brucei Family A mitochondrial DNA polymerases ……...5

2.1 Primers used for this study ……..11

LIST OF FIGURES

Figure Page

1.1 Diagram of the kDNA disk and its replication during T. brucei cell cycle ….... 9

3.1 TbIB-PTP single expresser cell line …… 27

3.2 Localization of POLIB-PTP during the cell cycle …….. 28

3.3 Characterization of POLIB-PTP signal ……... 29

3.4 Stability of POLIB-PTP following cycloheximide treatment ……. 30

3.5 Localization of POLIB-PTP with respect to TdT in situ labeling ……. 31

3.6 Characterization of POLIB-PTP at TdT in situ labeling …… 32

3.7 Quantitative fluorescence density plots ……...33

3.8 POLIB-PTP localization at the replicative stages ……. 34

3.9 Effect of POLIB silencing on POLIC-PTP …….. 35

3.10 POLIC-PTP localization when knocking down POLIB ……..... 36

3.11 POLIC protein levels during POLIB RNAi ……..... 37

4.1 Working models of T. brucei DNA mitochondrial polymerases localization during the cell cycle stages …… 42

CHAPTER 1

INTRODUCTION

1.1 *Trypanosoma brucei*

Human African trypanosomiasis (HAT), also known as African sleeping sickness is caused by the protozoan parasite, *Trypanosma brucei.* Two subspecies cause disease in humans, *T. brucei gambiense* and *T. brucei rhodesiense*. It is estimated that 70 million people are at risk of infection by this organism (Franco et al., 2014), mainly in the sub-Saharan Africa. The disease is differentiated by chronic and acute cases depending on the subspecies of the pathogen. 90% of HAT cases are caused by *T. b. gambiense* and present as a chronic disease with disease progression taking an average of 3 years while 10% of cases are caused by *T. b. rhodesiense* presenting an acute infection that can quickly proceed to death within 6 months if the patient is not treated. (Franco et al., 2014; WHO, 2010). A third subspecies, *T. brucei brucei* is strictly an animal pathogen causing the related wasting disease Nagana in cattle.

T. brucei is a vector transmitted disease with a complex life cycle. Multiple distinct morphological forms take place in both the insect vector, the tsetse fly (*Glossina* spp.) and in the mammalian host. An infection begins when an infected tsetse fly takes a blood meal, and injects parasites into the mammalian host. First stage of the disease is characterized mainly by intermittent fever due to replication of the parasite in the bloodstream and lymph. During the second stage of the infection, parasites cross the blood brain barrier and invade the central

nervous system causing neurological problems including disturbance to the sleep pattern of the patient. If left untreated, the infection proceeds to coma and eventually death due to the parasite's ability to continuously evade the host immune system via antigenic variation. Vector control using specialized tsetse fly traps can decrease the spread of the parasite. However, drug treatment is the main tool used to control the disease. No new medications have been developed over the last 3 decades which leaves the patient to rely on old, toxic and cumbersome intervenous treatments (WHO, 2010) (Table1). Identifying unique characteristics of *T. brucei* to provide newer more selective drug treatments is needed.

1.2 kDNA Structure

Like other eukaryotes, trypanosomes have typical organelles including a nucleus, Golgi apparatus, endoplasmic reticulum and mitochondria. The mitochondrial structure and accompanying DNA of trypanosomes is unique. Each parasite contains a single tubular branched mitochondrion that divides once every cell cycle as well as other single unit organelles like the flagellar basal body and the nucleus. The DNA is condensed into a disk-shaped DNA-protein structure in a specialized region of the mitochondrial matrix near the basal body, and consists of thousands of interlocked DNA rings called the kinetoplast DNA (kDNA) network (Jensen and Englund, 2012).

Medication	Year	Treat	Reference
Suramin	1916	First stage; *T. b. rhodesiense*	WHO, 2010
Pentamidine	1940	First stage; *T. b. gambiense*	WHO, 2010
Melarsoprol	1949	Second stage; both subspecies	WHO, 2010 Nok et al., 2003
Eflornithine	1990	Second stage; *T. b. gambiense*;	WHO, 2010 Burri et al., 2003
Eflornithine + nifurtimox	2009	Second stage; *T. b. gambiense*;	Gerardo et al. 2009

Table 1.1 Current treatments for human African trypanosomiasis.

The network contain two types of DNA rings, the minicircles (5000, 1 kb) and the maxicircles (25, 23 kb)(Jensen and Englund, 2012; Klingbeil et al., 2002; Liu et al., 2005). Maxicircles encode rRNAs and several proteins involved in energy transduction including subunits of cytochrome oxidase, NADH dehydrogenase, and ATP synthase (Jensen and Englund, 2012; Liu et al., 2005). Minicircles are heterogeneous in sequence but contain a conserved region known as the universal minicircle sequence that acts as an origin of replication. Minicircles encode guide RNA for the maxicircle post-transcriptional RNA editing process which is another unique feature in this organism (Guilbride and Englund, 1998). Additionally, the kDNA network has defined areas in which proteins localize and function to replicate the kDNA. Besides the disk itself, one area, the kinetoflagellar zone (KFZ), is located between the disk and the basal body (Figure 1.1A) and is where minicircle replication intermediates are first detected. The antipodal sites are two electron dense regions at opposite poles of the kDNA disk that contain numerous kDNA replication proteins and where replication intermediates are also detected.

1.3 kDNA replication and cell cycle progression

In order to avoid the topological complexity of the catenated kDNA network, replication proceeds by a mechanism of minicircle release and reattachment. The proposed model starts with the vectoral release of minicircles from the network by a topoisomerase II ($TopoII_{mt}$) in the KFZ where replication

Protein	Localization during the cell cycle	RNAi phenotype	Stability	Reference
Pol ID	Antipodal sites during kDNA S phase. Mitochondrial matrix during all other cell cycle stages.	Loss of kDNA	Proteolytic stable	Concepción-Acevedo, et al., 2012
Pol IC	KFZ at G1 phase. Antipodal sites during kDNA S phase. Undetected by fluorescence microscopy during G2/M and cytokinesis.	Small kDNA	Proteolytic stable	Concepción-Acevedo, et al.,unpublished
Pol IB	KFZ Dynamic localization not determined.	Loss of kDNA	Not determined	Klingbeil, et al., 2002
Pol IA	Mitochondrial matrix Dynamic localization not determined.	No phenotype	Not determined	Klingbeil, et al., 2002

Table 1.2 Trypanosoma brucei Family A mitochondrial DNA polymerases

initiates (Lindsay et al., 2008). Two proteins are associated with initiation steps, UMSBP and p38 (Abu-elneel et al., 2001). The antipodal sites were first characterized by the presence of several proteins involved in Okazaki fragment processing and gap filling, but now also contain proteins with other roles during various stages of kDNA replication. Interestingly, newly replicated minicircles that still contain a gap accumulate at these sites prior to reattachment to the network by Topo II (Wang and Englund, 2001). Once all minicircles have replicated the final gaps are filled in. Maxicircles have been studied in less detail, but these molecules replicate still attached to the network.

Since kDNA is a complex structure, it was hypothesized that its replication might require as many of 150 proteins. Approximately 30 proteins have been well characterized with regard to functions and localization (Jensen and Englund, 2012). This process requires multiple topoisomerases, primases, DNA polymerases, helicases, and ligases. While this multiplicity could reflect redundancy to ensure genome stability, the enzymes appear to have distinct roles in kDNA replication. The proteins have discrete localization patterns mainly in the antipodal sites and the KFZ suggesting an orchestration of replication proteins to complete replication of the network (Fig 1.1A).

Not only does kDNA network replication involve multiple proteins, the events must be coordinated with duplication of the other single unit organelles (basal body, nucleus) within the cell cycle (Gluenz et al., 2011). First, kDNA synthesis initiates immediately after duplication of the basal bodies. As newly

replicated molecules accumulate and reattach at the antipodal sites, the kDNA disk remains associated with the two basal bodies and will elongate to form a dome shape (Fig 1.1B, 1N1K$_{div}$). As the cell cycle progresses, the basal bodies migrate farther apart and the kDNA will appear bilobed and finally segregate into two new kDNA networks (Fig 1.1B,1N2K). These events occur prior to the completion of nuclear DNA S phase. Finally, mitosis occurs (Fig 1.1B, 2N2K) and then cytokinesis proceeds giving rise to two daughter cells.

1.4 Rationale and Objective

In contrast to mammalian mitochondria that contain a single DNA polymerase (Pol γ), *T. brucei* harbors multiple mitochondrial DNA polymerases Two are related to the nuclear DNA repair protein Pol β (TbPol β and TbPol β-PAK) and four are family A DNA polymerases related to bacterial DNA pol I (POLIA, POLIB, POLIC, and POLID) (Klingbeil et al., 2002; Saxowsky et al., 2003). Depletion of POLID, POLIC and POLIB via RNAi showed that these proteins are essential for kDNA replication and maintenance in both procyclic and bloodstream form parasites (Table 1.2) (Bruhn et al., 2011). As mentioned above, kDNA replication is spatially and temporally organized within a defined period of the cell cycle and timing of localization of the proteins involved in kDNA replication might be a way to regulate and coordinate this biological process. Interestingly, POLID and POLIC have dynamic localization during cell cycle progression (Table 1.2). During kDNA replication, these two proteins colocalize at

the antipodal sites and colocalize with replicating minicircles. Specifically, POLID localizes to the mitochondrial matrix but redistributes to the antipodal sites when the cells are undergoing kDNA replication (S phase). POLIC initially localizes in the KFZ prior to kDNA replication (G1 phase). As the cell cycle progression proceeds, POLIC is detected at the antipodal sites, and then become undetectable in later cell cycle stages (Concepcion-Acevedo et al., data unpublished). POLIB was previously reported to localized in the KFZ (Klingbeil et al., 2002), however the cell cycle dynamic of this localization pattern was never studied.

The purpose of the study is to identify POLIB localization throughout cell cycle progression, mainly using immunofluorescence microcopy as the prefer method. We hypothesize that since POLID and POLIC has a dynamic localization in the antipodal sites at kDNA replicating stage, that POLIB will also have a similar choreography. Additionally we will like to address if depletion of POLIB has any affect in protein levels and localization of other kDNA proteins. In this study, POLIC was chose for this kind of experiment since it seem that they have a similar localization near the kDNA when the trypanosomes are at a non-replicating stage (Fig 1.2, 1N1K).

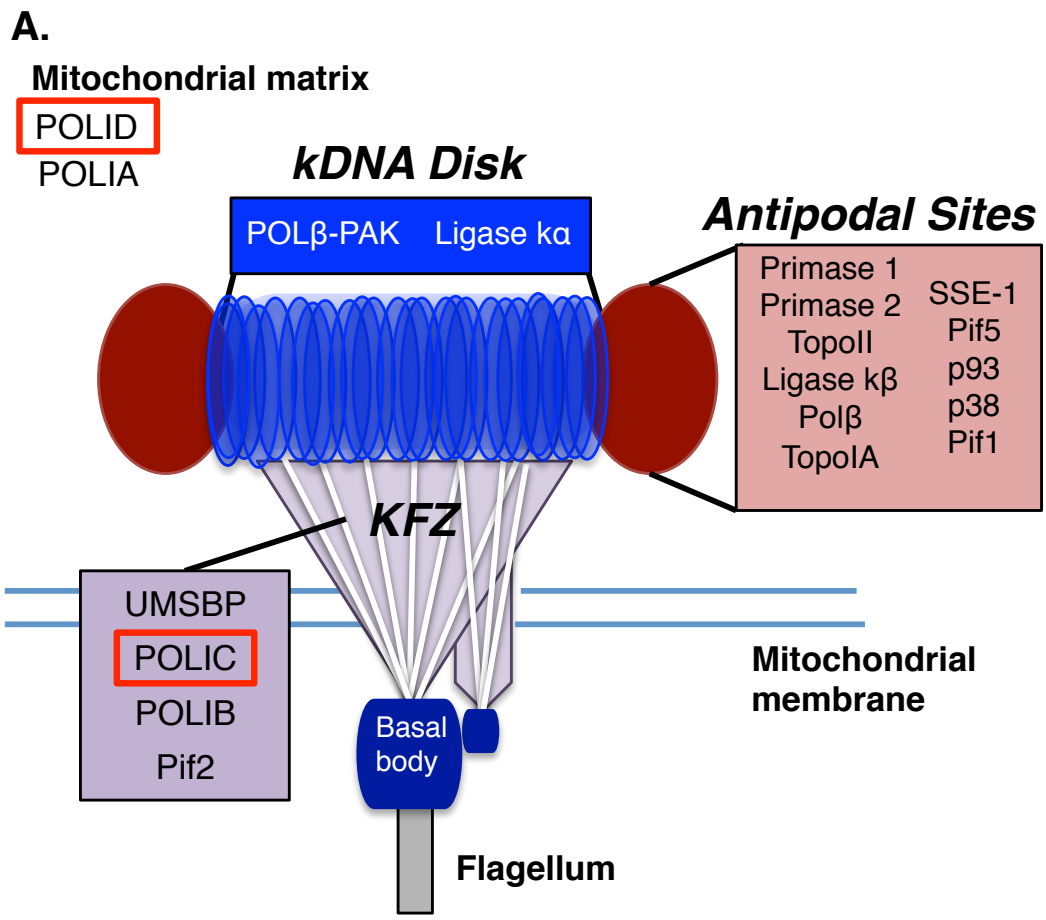

Figure 1.1 Diagram of the kDNA disk and its replication during *T. brucei* cell cycle. (A) Localization of critical kDNA replication proteins in the kDNA region. Red boxes, proteins that display dynamic localization in coordination with the cell cycle. POLIC and POLID localize to the antipodal sites during kDNA synthesis. (B) Representative images of different cell cycle stages in *T. brucei*. DAPI staining (blue) indicates the number and location of kinetoplasts (K) and nuclei (N). Basal body staining (magenta). During cell cycle progression, the basal body duplicates first followed by kDNA replication in near synchrony with nuclear DNA replication.

CHAPTER 2

MATERIALS AND METHODS

2.1 Plasmid constructs

2.1.1 POLIB-PTP chromosomal tagging construct

The POLIB C-terminal coding sequence (2261 bp) was PCR-amplified from *T. brucei* 927 genomic DNA using forward (MK351) and reverse (MK352) primers containing ApaI and EagI linkers, respectively (Table 2.1). The PCR-amplified fragment was ligated into ApaI and NotI restriction sites of pC-PTP-NEO (Schimanski and Gunzl, 2005) to generate the pPOLIB-PTP-NEO vector.

2.1.2 POLIB knockout construct

The pKO^{Puro} plasmid is a derivative of the $pKO^{NEO/HYG}$ series (Lamb et al., 2001). A 518 bp POLIB 5' UTR fragment was PCR amplified using forward (MK455) and reverse (MK456) primers containing XhoI and HindIII linkers respectively, and ligated into the corresponding pKO^{Puro}sites. Subsequently, a 314 bp POLIB 3' UTR fragment was PCR amplified using forward (MK457) and reverse (MK458) primers containing SpeI and XbaI linkers respectively, and ligated into the corresponding pKO^{Puro} sites to generate the $pKOPOLIB^{Puro}$ construct. After digestion with XhoI and XbaI, the 3047 bp fragment containing the Puromycin (Puro) resistance marker flanked by the POLIB UTRs was used for transfection into parasites.

Gene	Purpose	Primer Name	Primer Sequence	Linker
Tb POLIB	PTP tagging	MK351	5'-TTG TGT GGG CCC GGC TAT CGA CAA GTC TCT CTC TC-3'	ApaI
		MK352	5'- TGT TGT CGG CCG CAC CGT AAT TTC TAC ACT GTC-3'	EagI
	Single knockout	MK455	5'- TAT AGA CTC GAG GTT GTT GTT TGC CCA CCG TTC G -3'	XhoI
		MK456	5'- TAT AGA AAG CTT ATC ACT ATG CGG ACC ACC AG -3'	HindIII
		MK457	5'- TAT ATA ACT AGT GAC ATT CCC AGG TGT TAA GTT G -3'	SpeI
		MK458	5'- TAT ATA TCT AGA CAC TTC TGC CCT CGC CC -3'	XbaI
	qPCR	MK785	5'-GTG CGG AAC TTG CCC AAA TGA TGA-3'	-
		MK786	5'-TAT CCA CGC CAC AGT CCA CTG AAA-3'	-
Tb POLIC	qPCR	MK561	5'-ATG CTC TTT GTC CCA ACC CTC TCA-3'	-
		MK562	5'-ATG ATC CGG TTC CTC CCA CTG TTT-3'	-
Tb POLID	qPCR	MK559	5'-TGG CGA AAT CAT ACG GTG GTC AGA-3'	-
		MK560	5'- TGC GCG AGT GCT CGT TCT ATA TGT-3'	-
TERT	qPCR	MK804	5'-GAG CGT GTG ACT TCC GAA GG-3'	-
		MK805	5'-AGG AAC TGT CAC GGA GTT TGC-3'	-
PRF2	qPCR	MK806	5'-GAA GTT GAA GGT GTT GTG AGT CC-3'	-
		MK807	5'-CCT CCA GCG TGA TAT CTG TTA CC-3'	-

Table 2.1 Primers used in this study. List of primers used for epitope tagging, generating and confirming single allele knockout, and qPCR. Underlined region within the primer sequence corresponds to the position of the restriction enzyme linker.

2.2 Trypanosome growth and cell lines

2.2.1 Standard Growth Conditions

Procyclic *T. brucei* strain Lister 427 cells were cultured at 27°C and 5% CO_2 in SDM-79 containing 15% heat-inactivated fetal bovine serum (FBS). Transgenic cell lines were grown under the same conditions with the addition of the appropriate drug selection.

2.2.2 Generation of TbIB-PTP single expressor cell line

For POLIB-PTP single expressor cell lines, 427 WT cells were transfected by electroporation with the pKOPOLIB^{Puro} XhoI/XbaI fragment (3047 bp). A stable population was first selected with 1 µg/mL Puro, followed by limiting dilution as described previously (Bruhn et al., 2010). Clones were verified by southern blot analysis for proper chromosomal integration. The POLIB^{KO} clonal cell line P1C2 was then transfected with AatII linearized pPOLIB-PTP-NEO vector and the population was selected with 50 µg/mL G418 and 1 µg/mL Puro. Following limiting dilution cloning, clonal cell lines were analyzed for POLIB-PTP expression and proper chromosomal integration by Western and Southern blot analyses, respectively. The data presented in this study correspond to clonal cell line P2F11, which we named TbIB-PTP.

2.2.3 POLIC-PTP chromosomal tagging and POLIB RNA interference

The stem-loop vector pSLIB for POLIB RNAi was generated as previously

reported (Bruhn, Mozeleski, Falkin, and Klingbeil, 2010). The pPOLIC-PTP-PURO construct was stably integrated by transfection into a 29-13 cell line, as previously described (Bruhn, Mozeleski, Falkin, and Klingbeil, 2010). This clonal cell line was then transfected with NotI linearized pSLIB. Cells expressing POLIC-PTP and the intramolecular stem-loop RNA to target POLIB were subsequently transfected with pKOPOLIC^{BSR} for knockout of the POLIC wild type allele and selected with G418 (15 µg/ml), hygromycin (50 µg/mL), phleomycin (2.5 µg/mL), puromycin (1 µg/mL) and blasticidin (10 µg/mL) to generate the single expressor PTP-tagged POLIC allele. POLIC knockout was confirmed by PCR analysis. This cell line is referred to as POLIB^{RNAI}, POLIC$^{BSD/PTP}$.

2.3 Fluorescence Microscopy

2.3.1 Immunofluorescence (IF)

IB-PTP cells were harvested for 5 min at 1,000 x g, re-suspended in PBS, and adhered to poly-L-lysine (1:10) coated slides for 5 min. Cells were fixed for 5 min using 1.5% paraformaldehyde (PFA) and washed three times (5 min each) in phosphate-buffered saline (PBS) containing 0.1 M glycine (pH 7.4) followed by 0.1% Triton X-100 for 5 min to permeabilize the cells. Cells were then washed 3 times in PBS, followed by incubation with anti-protein A serum (Sigma) and rat monoclonal antibody YL1/2 (Abcam) together for 60 min and diluted 1:2,000 and 1:3,000, respectively, in PBS containing 1% bovine serum albumin (BSA). Cells were then washed 3 times in PBS containing 0.1% Tween-20 and incubated with

the secondary antibodies Alexa Fluor 488 goat anti-rabbit (1:100) and Alexa Fluor 594 goat anti-rat (1:250), respectively, in PBS containing 1% BSA for 1 hour. DNA was stained with 3 µg/mL 4'-6'-diamidino-2-phenylindole (DAPI), and slides were washed 3 times in PBS prior to mounting in Vectashield (Vector Laboratories).

2.3.2 *In situ* TdT labeling

Cells were fixed in 1.5% PFA, permeabilized in 0.1% of Triton X-100, and labeled with terminal deoxynucleotidyl transferase (TdT) as previously described (3). Briefly, cells were rehydrated in PBS and incubated for 20 min at room temperature in 25 µL of 2.5x TdT reaction buffer (Roche Applied Science) containing 2 mM $CoCl_2$. Cells were then labeled for 1 hour at room temperature in a 25 µL reaction solution (2.5x TdT reaction buffer, 2 mM $CoCl_2$, 10 µM dATP, 5µM AlexaFluor 594-dUTP, and 10 units of TdT). The reaction was stopped by the addition of 2x saline-sodium citrate (SSC). Slides were then processed for the localization of PTP-tagged proteins described above.

2.4 Image acquisition and analysis

2.4.1 Microscope and software

Images were acquired with a Nikon Eclipse E600 microscope using a Spot-RT digital camera and a 100x Plan Fluor 1.30 objective. Z-stack data were acquired using a Zeiss 200M inverted microscope equipped with a 63x lens. The

images were adjusted for brightness and contrast, analyzed and quantified using Image J (http://imagej.nih.gov/ij/).

2.4.2 Plot profile analysis

Plot profile analyses was performed using the strait line option from Image J tool bar. The line was placed either perpendicularly (from top to the bottom) or horizontally (from left to right) to the kDNA disk using the antipodal sites as the left, right orientation (See Fig 3.7). The plot profile tool was used for each channel (POLIB-PTP, TdT, DAPI) and pixel intensity (y axis) with length (x-axis) were plotted.

2.4.3 Surface plot analysis

Each kDNA disk was oriented so that the horizontal plane was viewed from left to right. Surface plot analysis from Image J analysis tool was then used for each channel and plotted separately and as a merged image (See Fig 3.7).

2.5 Western Blot analysis

Parasites were harvested at 3,500 x g for 10 min at 4°C and cell pellets were washed once in PBS supplemented with protease inhibitor cocktail. Cells were lysed in 4X SDS sample buffer and incubated at 94°C for 5 minutes. Proteins were separated by SDS-PAGE and transferred to PVDF membrane overnight at 90 mA in transfer buffer containing 1% methanol. The membrane

was blocked with 5% (w/v) milk for 60 min followed by incubation with antibodies diluted in 0.5% milk. PTP (Protein C-TEV-Protein A) tagged protein was detected with 1:2000 Peroxidase-Anti-Peroxidase soluble complex (PAP) reagent (Sigma), which recognizes the protein A domain of the PTP tag. For additional antibody detections, the membrane was stripped for 15 min with 0.1 M glycine (pH 2.5), washed in TBS with 0.1% Tween-20, blocked and re-probed with *C. fasciculata* specific Hsp70 antibody (1:7,500) (12) followed by secondary chicken anti-rabbit IgG-HRP (1:10,000). Detection of Cyc6-HA was done using anti-HA (1:1000) from Roche followed by secondary goat anti-mouse (1:1000). BM Chemiluminescence Western Blotting Substrate (POD) from Roche was used for protein detection.

2.6 Cycloheximide Treatment

Separate cell lines expressing POLIB-PTP and Cyc6-HA were incubated for 8 hours with 100 µg/mL cycloheximide in a side-by-side experiment. Cells were harvested every 2 hours and processed for Western Blot analysis, as described above.

2.7 POLIB RNAi

2.7.1 Cell growth and inductions

$POLIB^{RNAI}$, $POLIC^{BSD/PTP}$ cells were cultured at 27°C and 5% CO_2 in SDM-79 containing 15% heat-inactivated fetal bovine serum (FBS) and selection

drugs: G418 (15 μg/ml), hygromycin (50 μg/mL), phleomycin (2.5 μg/mL), puromycin (1 μg/mL) and blasticidin (10 μg/mL). Cells were induced for RNAi by adding 1 ug/ml tetracycline, and cell growth was monitored daily using a Z2 model Coulter (Beckman Coulter). To avoid variation in sample preparations, staggered RNAi inductions were performed to process all time points on the same day.

2.7.2 RNA isolation and quantitative PCR

Total RNA was harvested from 5 x 10^{7} uninduced and induced for RNAi for 48 hours cells at 4°C (3,500 rpm for 10 min). Pellets were washed with cold PBS and subsequently stored at -80°C. Thawed cell pellets were lysed using the TRIzol reagent (Ambion) according to manufacterer's protocol. RNA was treated with 10 units (30 min, 37°C) of RNase-free DNase I (BioRad) and subsequently cleaned using the RNA clean and concentrator kit (Zymo Research). The High Capacity cDNA Reverse Transcription Kit with RNase inhibitor (Ambion) and the Multi-Scribe Reverse Transcriptase were used to convert total RNA (500 ng) to cDNA. RT-PCR was performed in a 10 μL reaction containing 1 μL cDNA template, 5 μL 2X QuantiNova SYBR Green PCR Kit and 0.05 μL QN ROX Reference Dye (Qiagen), 300 nM each of forward and reverse primers, and nuclease-free water. Primers used for this analysis are listed in Table 2.1. qPCR was performed using the Mx3000P qPCR system (Agilent Technologies) and analyzed using the MxPro software. All data was normalized to telomerase

reverse transcriptase (TERT) and paraflagellar rod 2 (PFR2). The normalized values from induced samples were compared against uninduced controls for the relative expression levels of mRNA. Relative mRNA levels shown are represented as means of three experimental replicates.

CHAPTER 3

RESULTS

3.1 POLIB-PTP is seen in all cell cycle stages

Multiple DNA polymerases are involved in kDNA replication and maintenance, but the mechanism by which these DNA polymerases are spatially and temporally coordinated during kDNA replication stages remains largely unknown. Three of the DNA polymerase are essential for kDNA replication; POLIB, POLIC and POLID (Bruhn et al., 2010; Bruhn et al., 2011; Chandler et al., 2008; Klingbeil et al., 2002). Additionally, POLID and POLIC have dynamic localization during the cell cycle and even during the kDNA replication stages (Concepción-Acevedo et al., 2012; Concepción-Acevedo et al., unpublished). We hypothesize that the third essential kDNA polymerase, POLIB which was previously detected in the KFZ (Klingbeil et al., 2002), also displays dynamic localization during kDNA replication stages. We investigated the cell cycle localization of POLIB using an exclusive expressor cell line, TbIB-PTP, in which one allele was deleted and the other allele contained a PTP (Protein A–TEV–Protein C) epitope tag (Schimanski, et al., 2005) that was fused to the C-terminus. TbIB-PTP clonal cell lines (12 independent clones) were analyzed for POLIB-PTP expression, growth kinetics and kDNA morphology (data not shown). The data in this study was generated using clonal cell line P2F11. Using anti-protein A, POLIB-PTP was detected in all cell cycle stages in an unsynchronized

cell population (Fig 3.1). POLIB-PTP signal was always concentrated near the kDNA disk and could also be detected in the mitochondrial matrix. The kDNA associated signal varied displaying several patterns. In some cases the signal appeared concentrated in a single focus (Fig 3.1C, i) and in other instances the signal appeared more diffuse surrounding the kDNA disk (Fig 3.1C, ii).

T. brucei cell cycle progression can be monitored by DAPI staining and basal body labeling. The first detected events in the *T. brucei* cell cycle are the duplication of the basal body, followed closely by kDNA synthesis (Gluenz et al., 2011). Cells at the 1N1K stage (1 nucleus, 1 kinetoplast) will have one basal body and a single condensed structure for the kDNA disk. Just prior to kDNA replication a second basal body is formed and then the kDNA initiates synthesis shortly after ($1N1K_{div}$). At $1N1K_{div}$ the kDNA disk has two different structures: elongated or bilobe (Gluenz et al., 2011). Following replication, two kDNA disks segregate with their respective basal body (1N2K) and then replication of the nucleus completes. Cells undergo mitosis (2N2K) and produce two daughter cells.

To determine if POLIB-PTP signal variation is coordinated with specific cell cycle stages, we dually stained TbIB-PTP cells for POLIB-PTP (anti-protein A) and for basal body position using YL1/2 primary antibody and Alexa Fluor goat anti-rat 594 secondary antibody. YL1/2 is a marker for mature basal bodies in trypanosomes and is commonly used for the identification of cell cycle stages (Stephan et al., 2007). DAPI was used to evaluate the morphology of nuclear

DNA and the kDNA (Figure 3.2). POLIB-PTP foci were detected in all cell cycle stages, but in 1N1K and 1N1K$_{div}$ cells the signal also appeared more diffuse (Fig 3.2).

To examine these signals in more detail and determine if there was a cell cycle associated pattern, more than 300 intact cells were analyzed and characterized. Five major patterns could be classified (Fig 3.3A). In addition to a single focus and diffuse pattern, POLIB-PTP signal appeared to be segregated near the disk, or bilobed in shape as well as 2 separated foci detected only after the kDNA had segregated. For 1N1K cells, 30% of the cells had a single focus near the kDNA disk and 22% displayed a more diffuse pattern (Fig 3.3B). During 1N1K$_{div}$, the POLIB-PTP localization pattern displayed more variation with the single focus pattern decreasing to ~3% of the population. Cells with a diffuse pattern decreased slightly to 18% and 9% presented a segregated foci pattern. Lastly ~ 3% of cells also displayed a bilobe signal (Figure 3.3B). During G2/M stages (1N2K, 2N2K) the single focus and diffuse pattern were either greatly decreased or absent. Instead, the main pattern detected was two separated foci. The POLIB-PTP signal is detected near the kDNA disk at all cell cycle stages with varying patterns displayed across the cell cycle. Interestingly, the stage when kDNA is replicating (1N1Kdiv) displays the greatest number of patterns.

Although POLIB is always present, changes in protein abundance could account for the variation in signal pattern. To determine if proteolytic degradation plays a role in POLIB localization, POLIB-PTP proteins levels were monitored

after inhibiting protein synthesis using cycloheximide (CHX) treatment. Cells were harvested every 2 hours over an 8 hr time course and protein levels were monitored by immunoblot (Fig 3.4). POLIB protein levels were essentially unchanged during the CHX treatment while those of HA-tagged Cyclin 6 (CYC6) declined after 4 hrs of treatment and were nearly undetected after 8 hrs. These data demonstrate that POLIB is not regulated by proteolysis similar to three other *T. brucei* DNA polymerases, Polβ, POLIC and POLID (Concepción-Acevedo et al., 2012)

3.2 POLIB does not localize at the antipodal sites.

Minicircles are released from the kDNA disk via topoisomerase and replication is initiated in the KFZ. Newly gapped minicircles can be detected in the KFZ but are more easily visualized at the antipodal sites where they accumulate prior to reattachment to the disk (Drew and Englund, 2001). POLID and POLIC localize at the antipodal sites with newly replicated minicircle during kDNA synthesis. To distinguish the POLIB-PTP patterns in more detail, we analyzed whether POLIB localizes at the antipodal sites in a subset of the cells using terminal deoxynucleotidyl transferase (TdT) and a fluorescent deoxynucleoside triphosphate (dNTP) to *in situ* label newly synthesized minicircles that contain gapped regions.

The previously characterized multiple TdT labeling patterns were observed (Fig 3.5). During G1 (1N1K), cells contain a unit-sized kDNA that is TdT negative

(TdT-) as the minicircles (and maxicircles) are covalently closed with no gapped or nicked regions. During early stages of kDNA replication the antipodal sites are enriched with multiply gapped minicircles and show a strong TdT+ signal and then at later stages the gapped progeny are reattached to the network and the TdT signal is found within the kDNA disk. Although the POLIB-PTP signal was detected in all cells, the signal did not colocalize with early TdT+ label found at the antipodal sites. However, in later kDNA replication stages, POLIB-PTP signal appeared to partially overlap with the late TdT+ signal (Fig 3.5, merge and enlargements).

We were interested to determine the percentage of TdT+ cells and the corresponding POLIB-PTP pattern. In an unsynchronized population, 35% of cells were TdT- which is in agreement with previously published data (30-35% TdT-), while 30% of the population was TdT positive (1N1K_{div}). This could be further subdivided into Tdt+ early (25%) and Tdt+ late (5%) stages of kDNA replication (Fig 3.6A). We then proceeded to analyze the POLIB-PTP signal patterns in only 1N1K an 1N1K_{div} cells(Fig 3.6B).

POLIB-PTP signal was further analyzed during replicating stages (TdT+), using quantitative density plot profiles. For this analysis, both the signal along the perpendicular (line from top to bottom) and horizontal (line form left to right) planes of the kDNA disk were used to distinguish the POLIB-PTP signal relative to the kDNA disk (Fig 3.7). Analysis through the perpendicular plane allows determination if POLIB signal is seen near the disk (KFZ) or in the disk while

analysis across the horizontally plane is taking into consideration colocalization with the antipodal sites. Randomly selected cells were quantified at early TdT (10) and late TdT (5) stages (Fig 3.6). We characterized POLIB-PTP using the previously described nomenclature. In TdT- cells, 10 had a single POLIB-PTP focus and 9 contained the diffuse pattern. At early TdT+ stages, 7 out of 10 had a diffuse signal (Fig 3.6B), were the other 3 presented a single focus. For late TdT+, only 1 displayed a diffuse pattern while 4 out of 5 showed a segregated pattern (Fig 3.6B). We then used the perpendicular plot profile to identify if there is any colocalization in the late stages of TdT (figure 3.8). Three patterns were identified with POLIB-PTP in association with kDNA disk. 10 cells were near the disk, 7 overlap in and 2 in the disk at TdT-. During early TdT+, 6 out of 10 cells POLIB-PTP appeared to be partially in the kDNA and in 4 the signal was detected in the disk (Figure 3.8A). Interestingly, during late TdT+, 3 out of 5 cells were seen in the disk and two overlapping in the disk as oppose to early TdT. These data suggest that POLIB-PTP might be relocalizing to within the kDNA when replication of minicircles is nearing completion in contrast to POLIC and POLID that relocalize to the antipodal sites during kDNA synthesis.

3.3 Depletion of POLIB causes a reduction of POLIC-PTP

Localization of one kDNA polymerase could depend on the localization of another, and there is evidence accumulating to support this idea. When POLIB is depeleted by RNAi, POLIC-PTP proteins levels decline and the

localization pattern is disrupted. (Concepcion et al, unpublished). To explore if the dynamic localization of POLIC is also impacted by loss of POLIB, we generated a single expressor POLIC-PTP cell line that can also be induced for POLIB RNAi ($POLIB^{RNAi}$ $POLIC^{PTP/KO}$). To deplete the cells of POLIB, expression of a stemloop dsRNA is induced by adding tetracycline to the cells and the phenotype is analyzed over 8 days. POLIB knockdown caused growth inhibition starting a day that persisted through the 8 day induction in agreement with the previously published data on *TbPOLIB* silencing (Fig 3.9A) (Bruhn et al., 2010). Quantitative PCR analysis indicated that the relative amount of POLIB mRNA decreased by 70% after 2 days of POLIB RNAi with no significant changes in the mRNA levels of POLIC and POLID (Figure 3.9B).

To assess the effect of POLIB depletion on the kDNA disk, DAPI staining over the course of the RNAi induction showed that there was a progressive loss of kDNA starting at day 4, (Figure 3.9C), similar to published data (Bruhn et al., 2010). By day 4 of induction, cells with normal sized network decreased to 19%, where 72.9% presented cells with small kDNA and 7% no kDNA. At day 6, only 2.9% of cells showed normal kDNA, 56.6% did not have kDNA and 40% small kDNA. The percentage of cell with normal sized kDNA declined to less than 1% during the course of the induction while the percentage of cells containing small and no kDNA increased to 28.7% and 70%, respectively by day 8.

To identify if POLIB knockdown has any affect in POLIC-PTP localization, immunofluorescence of POLIC-PTP and TdT labeling of the cells was performed.

PolIC-PTP signal decreased throughout a POLIB RNAi induction (Fig 3.10). Initially, POLIC localized at the antipodal sites at kDNA S phase (uninduced cells). Upon POLIB depletion, POLIC-PTP localization was detected only in cells that were TdT+. In TdT- cells, POLIC-PTP signal was either disorganized (D6) or completely absent (D4, D8). These data indicate than when POLIB levels are depleted, POLIC-PTP signal is disrupted.

To identify if proteins levels were impacted, whole cell extracts from uninduced and each day of POLIB depletion were analyzed by western blot (Fig 3.11A). The intensity of the bands were analyzed in Image J and normalized to the Hsp70 signal (Fig 3.11B). POLIC-PTP protein amounts decreased approximately 5% after 2 days of POLIB silencing and remained at this level until day 8 where there was a consistent 76% decline in POLIC-PTP protein. With these results we can conclude that POLIB depletion affects POLIC stability. It is not clear whether the impact on protein levels and localization is a direct or an indirect effect.

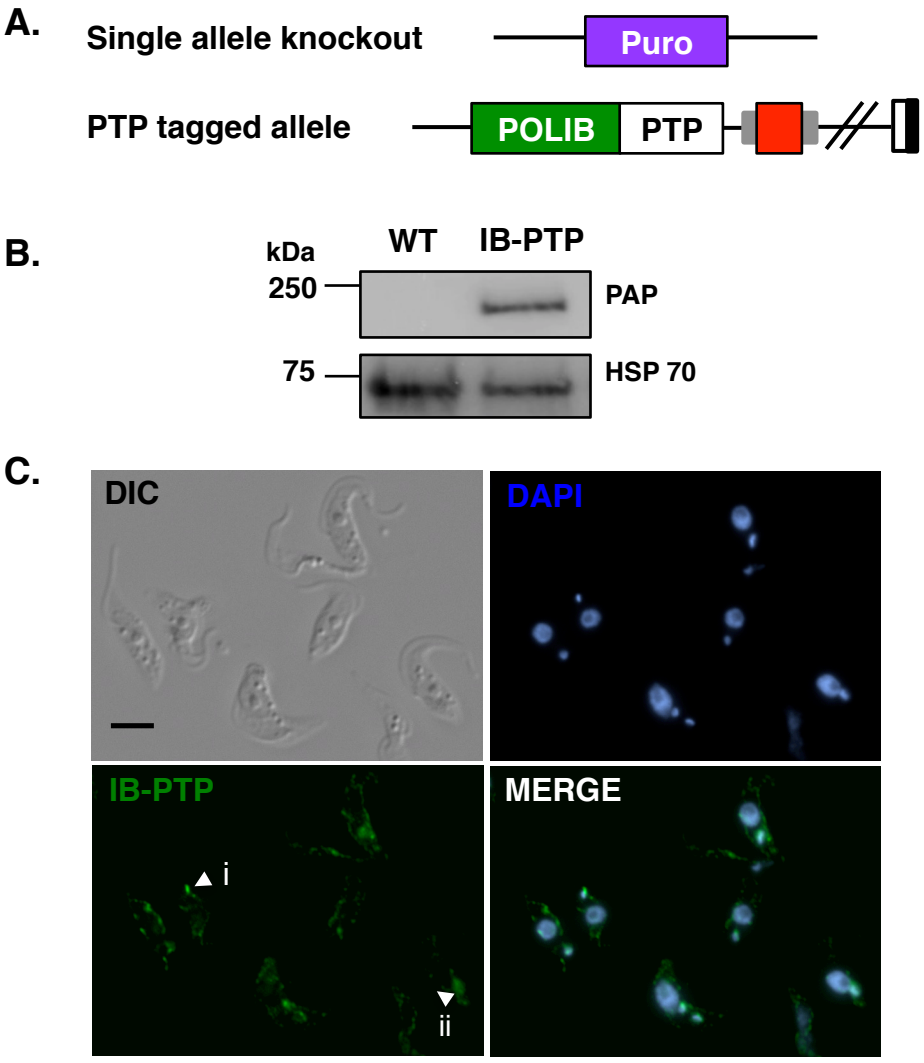

Figure 3.1 TbIB-PTP single expressor cell line. (A) Diagram representing the TbPOLIB gene locus in clonal cell line TbIB-PTP (not to scale). The POLIB coding sequence (green) was replaced in one allele with a puromycin resistance cassete (PURO), and in the second allele the PTP sequence was fused to the 3' end of POLIB by targeted insertion of the pPOLIB-PTP-NEO construct. (B) Western blot analysis of whole cell extracts (5 x 10^6 cells/lane) of wild type (WT) and TbIB-PTP cells. Tagged protein was detected with PAP reagent and HSP70 was used a loading control. (C) Localization of POLIB-PTP in an unsynchronized population. POLIB-PTP was detected using anti-protein A (green), and DNA was stained with DAPI (blue). White arrowheads indicate POLIB-PTP signals near the kDNA disk; i, single focus and ii, diffuse signal. Scale bar, 5µm.

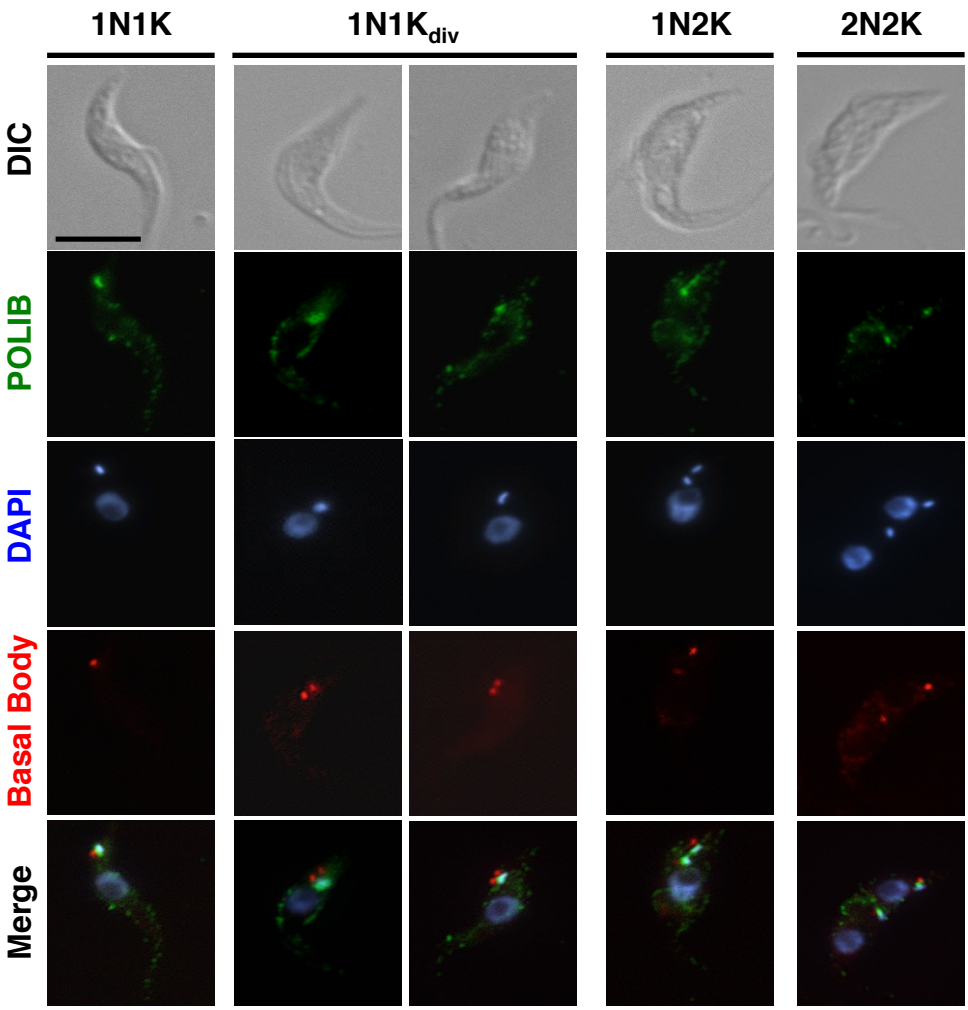

Figure 3.2. Localization of POLIB-PTP during the cell cycle. Representative cells from an unsynchronized population. TbIB-PTP cells were dually labeled with anti-protein A that detects POLIB-PTP (green) and YL1/2 (red) for detection of basal bodies, an indicator of cell cycle progression. DNA was stained with DAPI (blue). Scale bar, 5µm.

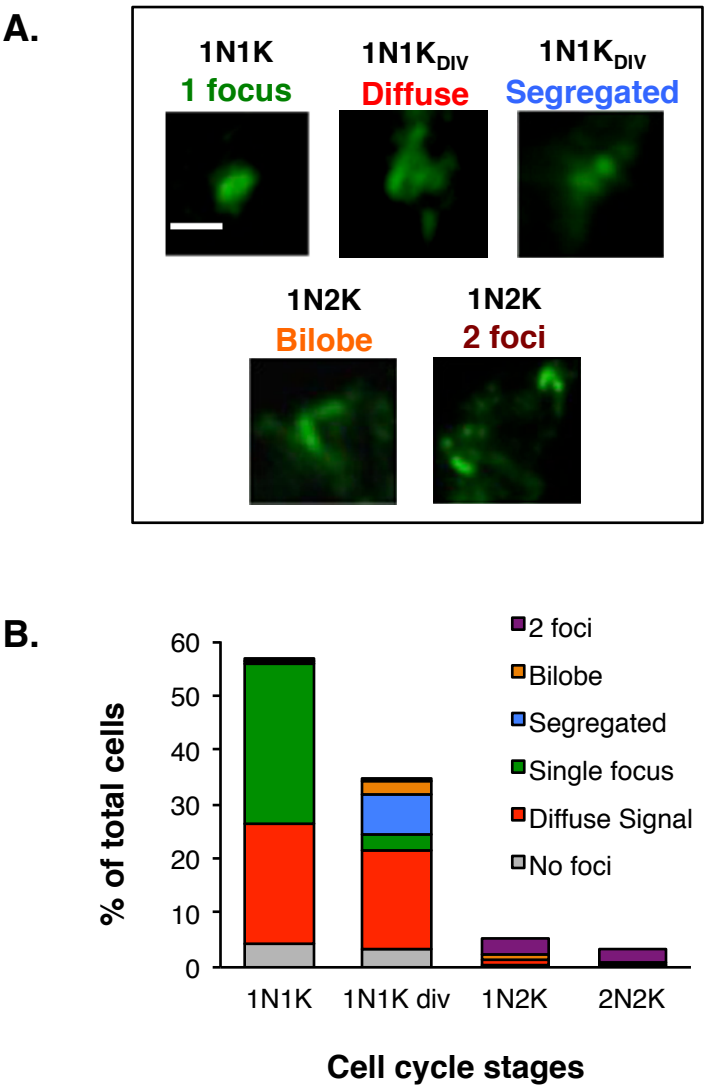

Figure 3.3 Characterization of POLIB-PTP signal. (A) Representative POLIB-PTP images selected. Enlarged patterns of POLIB-PTP signal detected during cell cycle progression. (B) TbIB-PTP cells were dually labeled with anti-protein A that detects POLIB-PTP (green) and YL1/2 for the detection of basal body. DNA was stained with DAPI. Distribution of POLIB-PTP patterns in an unsynchronized cell population. Individual cells were classified based on their kDNA morphology, basal body positioning and POLIB-PTP pattern. More than 300 cells were analyzed. Scale bar, 1.5µm.

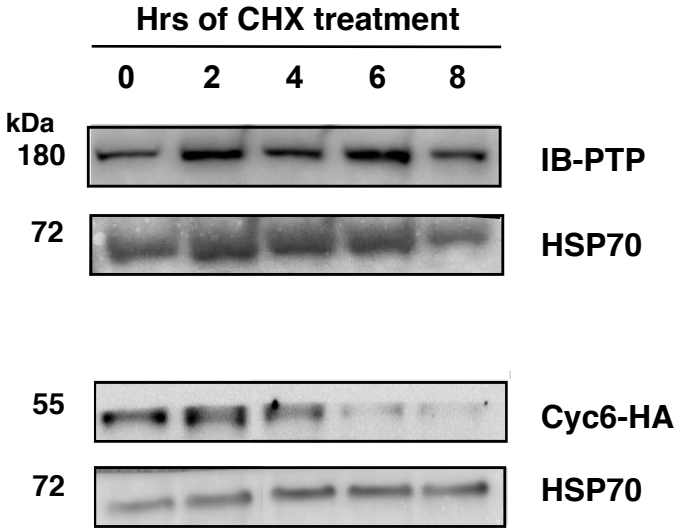

Figure 3.4 Stability of POLIB-PTP following cycloheximide treatment. Cyc6-HA cell line was used as a positive control. Following cycloheximide (CHX) addition, cells were harvested every 2 hours for a total of 8 hours. Whole cell extracts (5 x 10^6 cells) were analyzed by western blot analysis. Membrane was detected with PAP (IB-PTP), anti-HA (Cyc6), and anti-Hsp70.

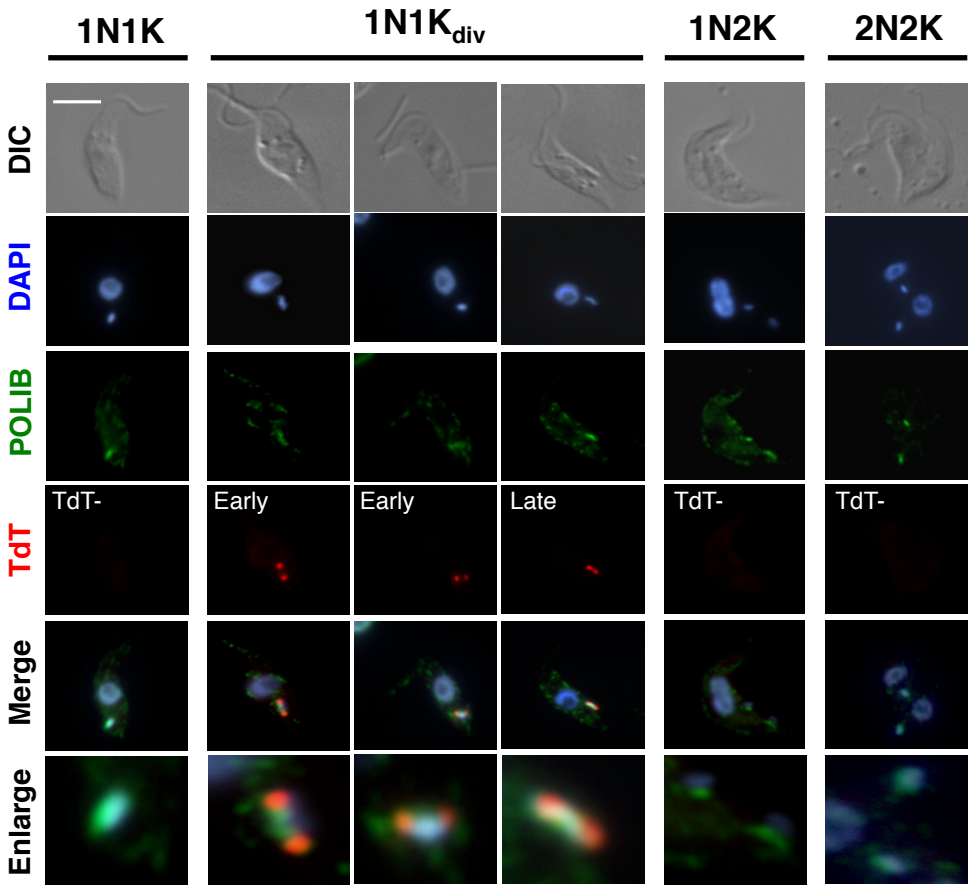

Figure 3.5 Localization of POLIB-PTP with respect to TdT *in situ* labeling. Localization of POLIB-PTP (green) following *in situ* TdT labeling (red). Representative images for TdT labeling patterns are shown (TdT-, Early, Late). Enlargements of the merged row focus on the kDNA disk to visualize colocalization. Scale bar 5µm.

A.

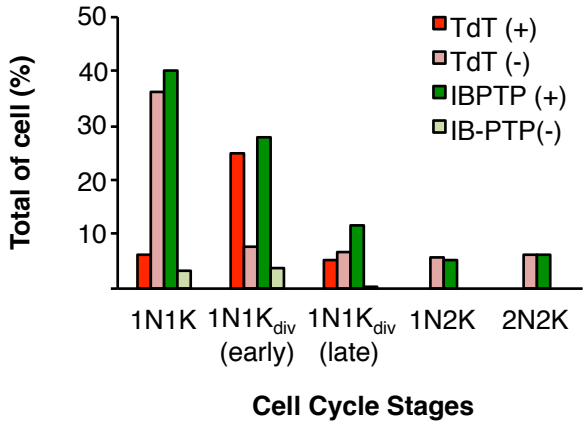

B.

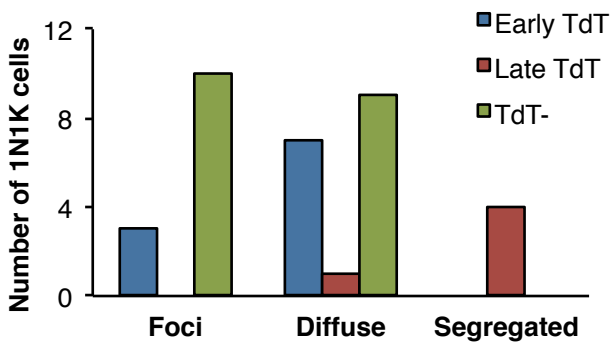

Figure 3.6 Characterization of POLIB-PTP at TdT *in situ* labeling. (A) Distribution of POLIB-PTP signal in a population of TdT labeled cells. Individual cells were also classified based on kDNA morphology. (B) Randomly selected cells (total of 34) in either 1N1K or 1N1K$_{DIV}$ stages were further subdivided into POLIB-PTP subcategories based on the signal pattern per cell.

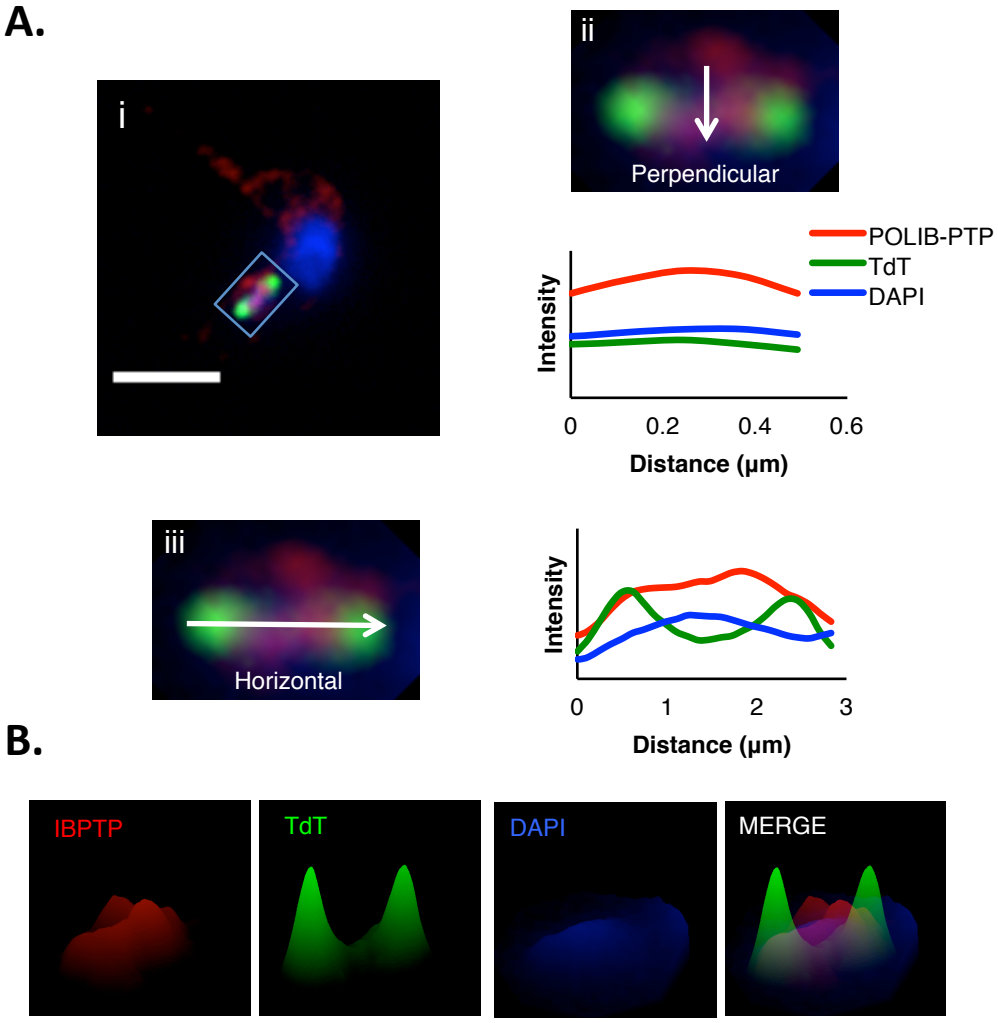

Figure 3.7 Quantitative fluorescence density plots. (A) Representative image of early TdT labeled network (i). Boxed region corresponds to enlargement viewed in ii and iii. The data for the Profile plot analysis graphs (IB-PTP, red; TdT label, green; DAPI, blue) were taken from a perpendicular section (ii) and a horizontal section (iii) of the image indicated by the white arrow. (B) Surface plot analysis of representative image (i) with early TdT labeling using a horizontal plane to evaluate. Scale bar is 5 μm.

A.

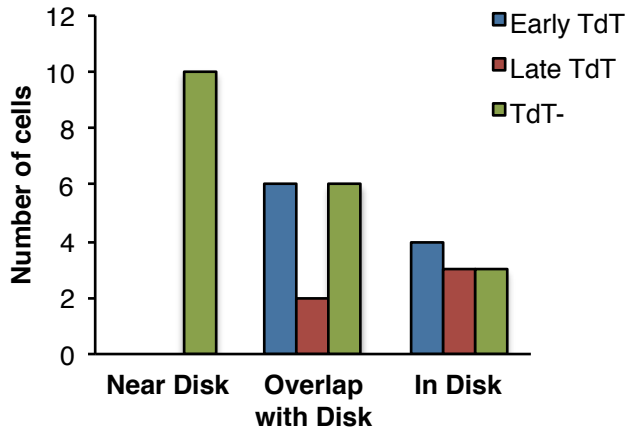

B.

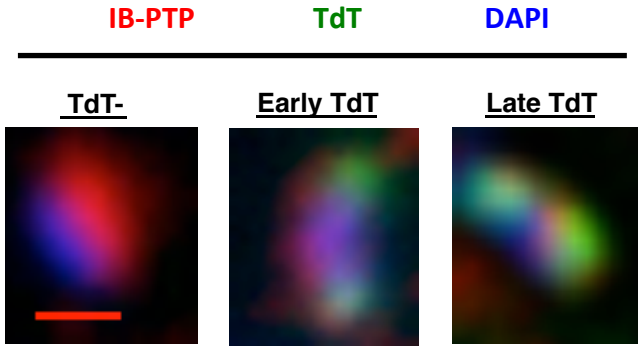

Figure 3.8 POLIB-PTP localization at the replicative stages. (A) Number of cells from negative (TdT-), early and late minicircles replication. Cells were classified as near, overlap in or in the disk using plot profile analysis along the perpendicular plane of the kDNA disk. (B) Representative merged images of TdT -, early TdT+ and late TdT+. POLIB-PTP (red), TdT labeling (green) and the kDNA (blue). Scale bar is 1 µm.

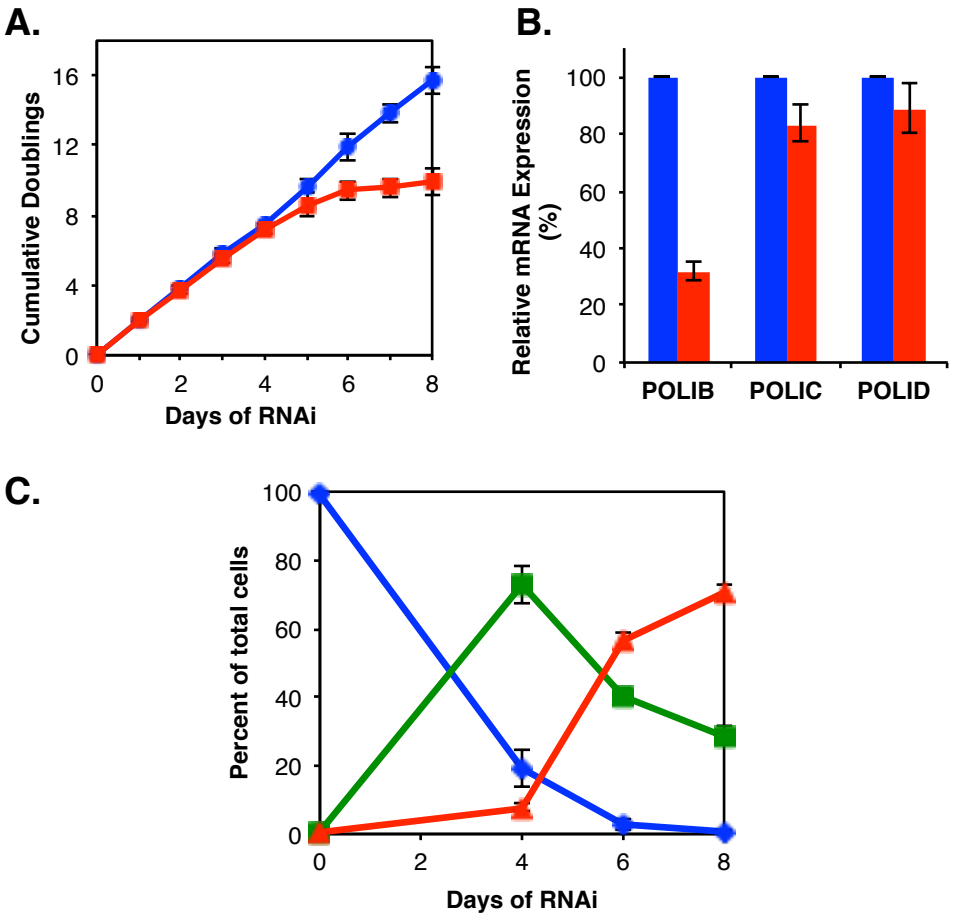

Figure 3.9 Effect of POLIB silencing on POLIC-PTP. (A) POLIB^{RNAi} POLIC$^{PTP/KO}$ clonal cell line was grown in the absence (blue) or presence (red) of tetracycline (1 ug/ml) to express the *TbPOLIB* stem-loop dsRNA. Cell density was plotted as cumulative doublings. Values represent the mean of four independent RNAi inductions. (B) Relative expression of *TbPOLIB*, *TbPOLIC* and *TbPOLID* mRNA levels following 48 hr of TbPOLIB RNAi were analyzed by qRT-PCR using TERT and PFR2 as normalizers. Values represent the mean from four individual experiments. Error bars represent standard deviation. (C) Kinetics of kDNA loss. DAPI-stained cells (200 cells per time point) were scored for normal sized kDNA (blue circles), small kDNA (green squares) or no kDNA (red triangles). Values represent the mean from three independent experiments. Error bars represent the SEM.

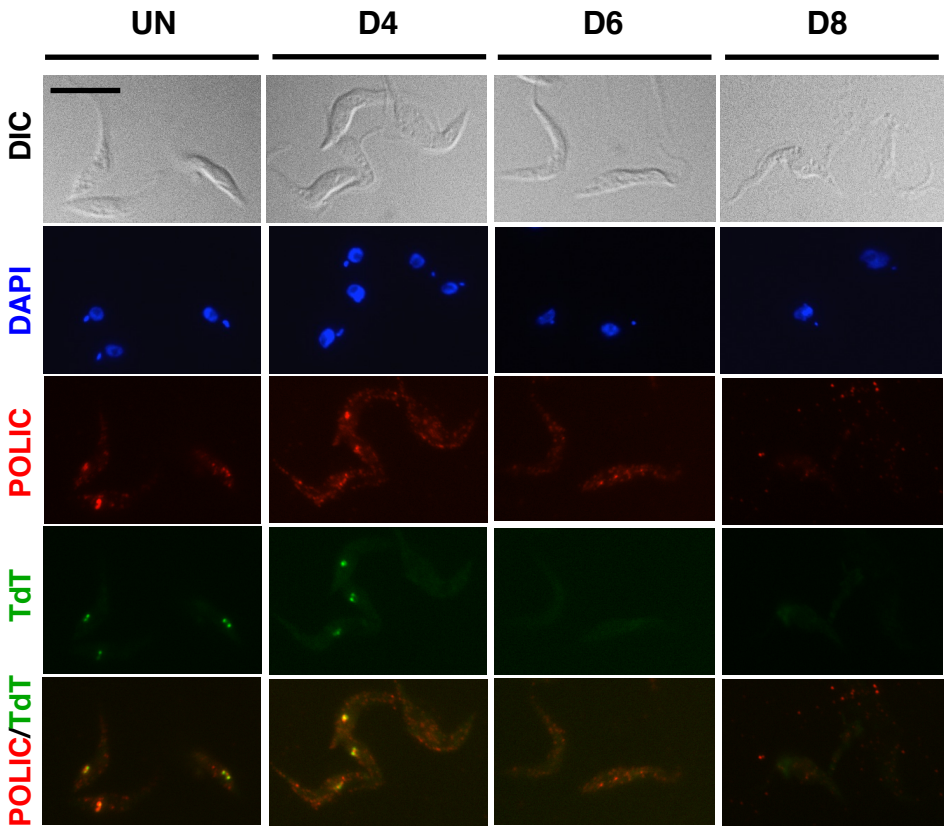

Figure 3.10 POLIC-PTP localization when knocking down POLIB. Detection of POLIC-PTP (red) and TdT-positive cells (green) during POLIB silencing during a RNAi by a course of eight days. Scale bar is 10µm.

A.

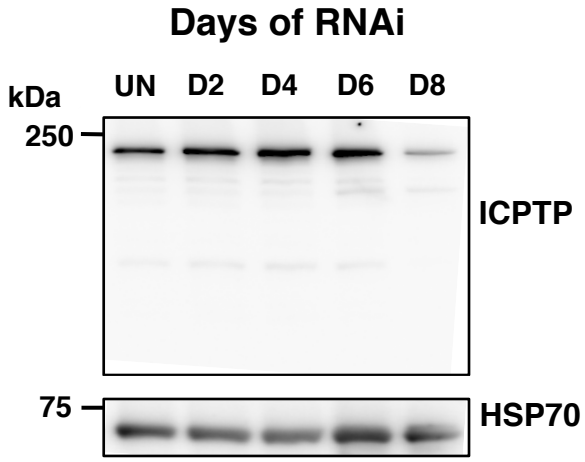

B.

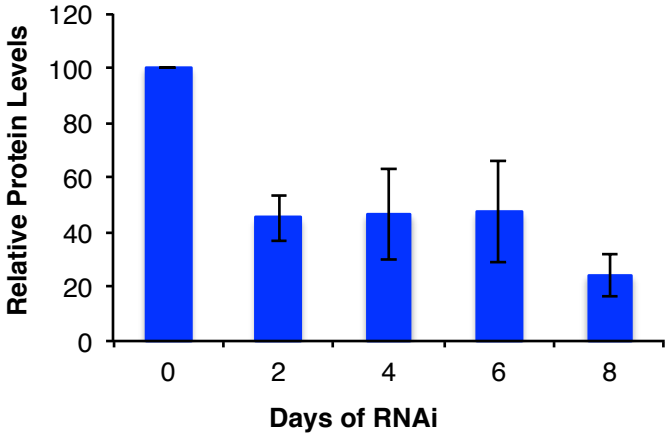

Figure 3.11 POLIC protein levels during POLIB RNAi. (A) POLIC-PTP and Hsp70 protein levels following POLIB RNAi. $POLIB^{RNAi}$ $POLIC^{PTP/KO}$ cells were harvested at indicated times, and $5x10^6$ cells were loaded into each lane. (B) The number of pixels for each band was measured and normalized against the HSP70 signal using ImageJ. The graph represents data from three separate RNAi inductions.

CHAPTER 4

DISCUSSION

Replication of the kDNA network is a complex process. This complexity is based on that Trypanosomes have multiples proteins with similar activities but with different functions (Jensen & Englund, 2012). One example of the multiplicity is the presence of at least six mitochondrial DNA polymerases. POLIB, IC, and ID are known to be essential for kDNA replication in both procyclic and bloodstream form parasites (Bruhn et al., 2010; Bruhn et al. 2011; Chandler et al,, 2008; Klingbeil et al., 2002). However, the localization of these proteins differs with respect to the known kDNA regions. POLID is found in the mitochondrial matrix and POLIC at the KFZ in most of the cell cycle stages except when the kDNA is undergoing replication ($1N1K_{div}$). During this synthesis stage the two DNA polymerases precisely colocalize at the antipodal sites during the earliest kDNA synthesis stages. However, at later stages (when the disk is domed shaped and preparing for segregation) POLIC and POLID exhibit only partial colocalization. This shows that one way to regulate kDNA replication is by dynamic localization of these proteins. Since POLID and POLIC display dynamic localization, in this project we wanted to examine if POLIB also changes its localization during cell cycle stages, and whether it shares a location pattern with either of the other essential DNA polymerases during kDNA S phase.

To answer this question, a POLIB-PTP single expressor cell line was

constructed to characterize the localization of the protein throughout the cell cycle. Unlike POLIC and POLID, POLIB was seen in all cell cycle stages near the kDNA disk and 5 different signal patterns were identified (Fig 3.3). Although two patterns were dominant in the 1N1K stage (focus and diffuse), the $1N1K_{div}$ stage displayed all five patterns with the diffuse signal representing the major pattern. Bilobe, and 2 seperated foci were detected only at 1N2K and 2 foci for 2N2K. The change in patterns suggests that POLIB reorganizes during when kDNA is undergoing replication. Proteolytic degradation by HslVU plays a major role in regulating one of the kDNA helicases, Pif2 (Liu et al., 2009). However, there is no evidence that POLIC, POLID or Polβ are regulated by this mechanism as they were stable when protein translation was blocked by cycloheximide treatment. Likewise, POLIB is also resistant to proteolytic degradation under the conditions tested and therefore protein abundance does not appear to play a major role in regulating any of the changes seen in POLIB localization patterns (Concepción-Acevedo et al., 2012, Concepción-Acevedo et al., unpublish data).

TdT labeling is used to see the gaps of newly replicated minicircles at the antipodal sites. POLIB-PTP signal did not colocalize with early TdT. However, POLIB-PTP appeared to be overlapped with late TdT signal seen in the kDNA disk because of the minicircles getting incorporated into the disk. Further analysis of the subpopulation of early and late TdT identified two previous patterns described, diffuses and segregated. This results correlate with the quantification of an unsynchronized population since the main patterns seen in

$1N1K_{div}$ were these ones in particular. Interestingly, diffuse pattern was mostly seen at early TdT and segregate at late TdT.

We clarified POLIB-PTP localization at $1N1K_{div}$ using a more quantitative approach known as plot profile analysis, a two-dimensional graph for pixel intensity and the length of region of interest, in this case the kinetoplast. Individual example of the kDNA disk were analyzed perpendicularly and horizontally and identified that at an early TdT POLIB-PTP was seen overlap in the disk. Interestingly, during late TdT stages the signal mainly segregated is seen in the disk. These results suggest that POLIB may be relocalizing into the kDNA disk after completion of minicircles replication and reattachment but prior to the phase when the last remaining gaps are filled in prior to network segregation. Intriguingly by the time the new network segregate (1N2K), the POLIB signal appears near the disk again as 2 separated foci.

Protein levels of POLIC were investigated in a POLIB stem-loop RNAi vector in which a single expressor POLIC-PTP tagged was transfected. Decrease in cumulative doubling, and progressive loss of kDNA were similar to the parental cell line (Bruhn et al., 2010). Protein levels of POLIC when POLIB was knockdown decrease have of half of the protein and remains constant for four days until more than half of the POLIC protein levels drop by day 8. Even though we checked mRNA expression at day 2 and no significant effect was seen in POLIC level, we cannot conclude that the decrease of POLIC is not cause by regulation in the transcription since we did not checked for mRNA expression

through a course of an RNAi.

By using the working model of kDNA replication we can assume or hypothesize what is the role of POLIB. At G1 (1N1K) POLIB is localize in the KFZ as well as POLIC (Figure 4.1). As minicircles start S-phase ($1N1K_{div}$), POLIB is getting reorganize (diffuse pattern) and start moving to the kDNA disk in contrast to POLIC and POLID that relocalize to the antipodal sites. Minicircles will start getting incorporated in which POLIB is seen in the kDNA disk, as well. Finally at G2 (1N2K) POLIB relocalize back to the kDNA.

Why might POLIB move into the disk at later stages of kDNA replication? There are several possibilities. First, it is known that maxicircle replication occurs late in the network replication stages after the bulk of minicircle replication (Ferguson et al., 1994). None of the mitochondrial DNA polymerases have been directly shown to impact just maxicircle replication. Second, POLIB could have a DNA repair function in which POLIB would proofread the minicircles prior to segregation of the new kDNA networks. This findings support that spatiotemporal localization in the kDNA network is fundamental for its maintain. Further studies need to be done to really understand POLIB specific function in the kDNA, but these observations will help decipher how this can be achieve.

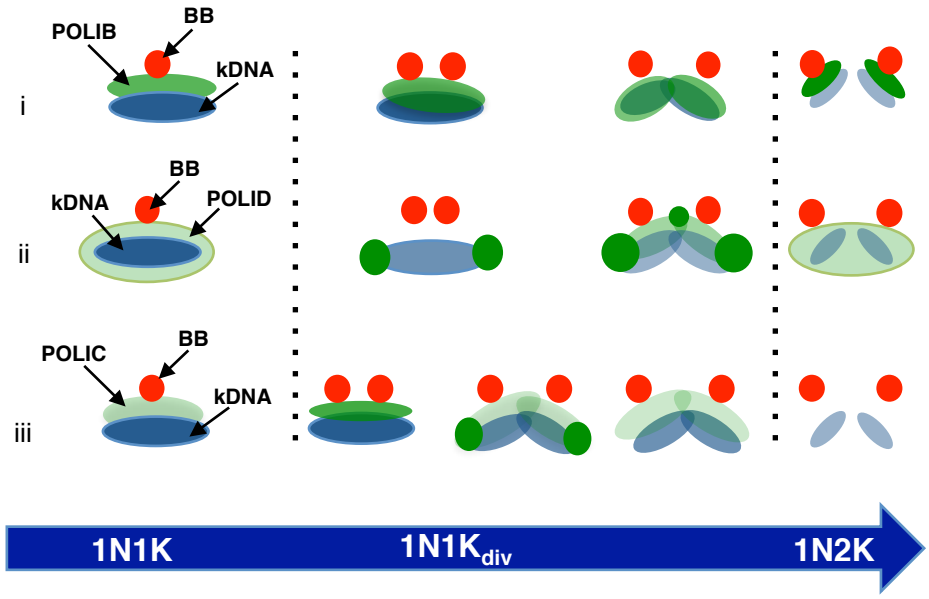

Figure 4.1 Working models of *T. brucei* DNA mitochondrial polymerases localization during the cell cycle stages. Three individual diagrams representing each polymerase (green), kDNA(blue), and basal body(red). (i) POLIB at 1N1K is seen at the KFZ. Then it move to the kDNA disk at 1N1K$_{div}$ and is seen back in the KFZ at 1N2K. (ii) POLID localized throughout the mitochondrial matrix (MM) at 1N1K, and relocalized in the antipodal sites at 1N1K$_{div}$. In 1N2K POLID is at the MM. (iii) POLIC is at the KFZ at a lower concentration in 1N1K and relocalized to the antipodal sites at 1N1K$_{div}$. POLIC is undetected at 1N2K.

REFERENCES

1. Abu-elneel, K., Robinson, D. R., Drew, M. E., Englund, P. T., & Shlomai, J. (2001). Intramitochondrial Localization of Universal Minicircle Sequence-binding Protein , a Trypanosomatid Protein that Binds Kinetoplast Minicircle Replication Origins, *153*(4), 725–733.

2. Bruhn, D. F., Mozeleski, B., Falkin, L., & Klingbeil, M. M. (2010). Mitochondrial DNA polymerase POLIB is essential for minicircle DNA replication in African trypanosomes. *Molecular Microbiology*, *75*(February), 1414–1425.

3. Bruhn, D. F., Sammartino, M. P., & Klingbeil, M. M. (2011). Three mitochondrial DNA polymerases are essential for kinetoplast DNA replication and survival of bloodstream form Trypanosoma brucei. *Eukaryotic Cell*, *10*(6), 734–43.

4. Chandler, J., Vandoros, A. V, Mozeleski, B., & Klingbeil, M. M. (2008). Stem-loop silencing reveals that a third mitochondrial DNA polymerase, POLID, is required for kinetoplast DNA replication in trypanosomes. *Eukaryotic Cell*, *7*(12), 2141–6.

5. Concepción-Acevedo, J., Luo, J., & Klingbeil, M. M. (2012). Dynamic localization of Trypanosoma brucei mitochondrial DNA polymerase ID. *Eukaryotic Cell*, *11*(7), 844–55.

6. Ferguson, L., Torri, A. E., & Ward, D. C. (1994). Kinetoplast DNA Replication : Mechanistic Differences between Trypanosoma brucei and Crithidia fasciculata, *126*(3).

7. Franco, J. R., Simarro, P. P., Diarra, A., & Jannin, J. G. (2014). Epidemiology of human African trypanosomiasis. *Clinical Epidemiology*, *6*, 257–75.

8. Gluenz, E., Povelones, M. L., Englund, P. T., & Gull, K. (2011). The kinetoplast duplication cycle in Trypanosoma brucei is orchestrated by cytoskeleton-mediated cell morphogenesis. *Molecular and Cellular Biology*, *31*(5), 1012–21.

9. Guilbride, D. L., & Englund, P. T. (1998). The replication mechanism of kinetoplast DNA networks in several trypanosomatid species. *Journal of Cell Science*, *111 (Pt 6*, 675–679.

10. Jensen, R. E., & Englund, P. T. (2012). Network news: the replication of kinetoplast DNA. *Annual Review of Microbiology*, *66*, 473–91.

11. Klingbeil, M. M., Motyka, S. A., & Englund, P. T. (2002). Multiple mitochondrial DNA polymerases in Trypanosoma brucei. *Molecular Cell*, *10*, 175–186.

12. Lindsay, M. E., Gluenz, E., Gull, K., & Englund, P. T. (2008). A new function of Trypanosoma brucei mitochondrial topoisomerase II is to maintain kinetoplast DNA network topology, *70*(October), 1465–1476.

13. Liu, B., Liu, Y., Motyka, S. a, Agbo, E. E. C., & Englund, P. T. (2005). Fellowship of the rings: the replication of kinetoplast DNA. *Trends in Parasitology*, *21*(8), 363–9.

14. Liu, B., Wang, J., Yaffe, N., Lindsay, M. E., Zhao, Z., Zick, A., Englund, P. T. (2009). Article Trypanosomes Have Six Mitochondrial DNA Helicases with One Controlling Kinetoplast Maxicircle Replication. *Molecular Cell*, *35*(4), 490–501.

15. Nok, AJ. (2003). Arsenical (melarsoprol), pentamidine and suramin in the treatment of human african trypanosomiasis. *Parasitology Research*, *90*(1), 71-9.

16. Priotto, Gerardo et al. (2009). Nifurtimox-eflornithine combination therapy for second-stage African Trypanosoma brucei gambiense trypanosomiasis: a multicentre randomised, phase III, non-inferiority trial. *The Lancet*, *374*(9683), 56-64.

17. Saxowsky, T. T., Choudhary, G., Klingbeil, M. M., & Englund, P. T. (2003). Trypanosoma brucei has two distinct mitochondrial DNA polymerase beta enzymes. *The Journal of Biological Chemistry*, *278*(49), 49095–101.

18. Schimanski B, Nguyen TN, Gunzl A. 2005. Highly efficient tandem affinity purification of trypanosome protein complexes based on a novel epitope combination. Eukaryot Cell 4:1942–1950.

19. Schimanski B, Nguyen TN, Günzl A, Gu A. 2005. Highly Efficient Tandem Affinity Purification of Trypanosome Protein Complexes Based on a Novel Epitope Combination Highly Efficient Tandem Affinity Purification of Trypanosome Protein Complexes Based on a Novel Epitope Combination. Eukaryotic cell 4:1942–50.

20. Shapiro TA, Englund PT. 1995. The structure and replication of kinetoplast DNA. Annu Rev Microbiol 49:117–43.

21. Shapiro TA, Showalter AF. 1994. In vivo inhibition of trypanosome mitochondrial
topoisomerase II: effects on kinetoplast DNA maxicircles. Mol Cell Biol 14:5891–5897.

22. Siegel TN, Hekstra DR, Cross GAM. 2008. Analysis of the Trypanosoma brucei cell cycle by quantitative DAPI imaging. Molecular and Biochemical Parasitology 160:171–4.

23. Wang, Z., & Englund, P. T. (2001). RNA interference of a trypanosome topoisomerase II causes progressive loss of mitochondrial DNA, *20*(17).

24. WHO. (2010). First WHO report on neglected tropical diseases: working to overcome the global impact of neglected tropical diseases. *World Health Organization*, 1–184.